arXiv:astro-ph/0010573v1 27 Oct 2000

The $z = 0.0912$ and $z = 0.2212$ Damped Lyα Galaxies Along the Sight-Line Toward the Quasar OI 363[1]

David A. Turnshek,[2] Sandhya Rao,[2] Daniel Nestor,[2] Wendy Lane,[2,3] Eric Monier[2,4]

Department of Physics & Astronomy, University of Pittsburgh, Pittsburgh, PA 15260, USA

Jacqueline Bergeron,[2]

ESO, Karl-Schwarzschild-Strasse 2, Garching bei Munchen, D-85748, Germany

and

Alain Smette[2]

NASA Goddard Space Flight Center, Code 681, Greenbelt, MD 20771, USA

ABSTRACT

New optical and infrared observations along the sight-line toward the quasar OI 363 (0738+313) are presented and discussed. Excluding systems which lack confirming UV spectroscopic observations of the actual Lyα line, this sight-line presently contains the two lowest-redshift classical damped Lyα (DLA) quasar absorption line systems known (i.e. with $N_{HI} \geq 2 \times 10^{20}$ atoms cm^{-2}), one at $z_{abs} = 0.0912$ and the other at $z_{abs} = 0.2212$. Our new observations suggest identifications for the DLA galaxy counterparts of these absorption-line systems. The $z = 0.09$ DLA galaxy appears to be an extended low surface brightness galaxy which is easily visible only in infrared images and shows rich

[1]Based on observations obtained with the Mayall 4.0-m NOAO Telescope on Kitt Peak, operated for NSF by AURA, the 3.5-m WIYN Telescope on Kitt Peak, also operated for NSF by AURA (WIYN is a joint facility of University of Wisconsin, Indiana University, Yale University, and NOAO), the NASA 3.0-m IRTF on Mauna Kea, operated for NASA by University of Hawaii, and the Hiltner 2.4-m Telescope on Kitt Peak, operated by MDM Observatory (this is a joint facility of University of Michigan, Dartmouth College, Ohio State University, and Columbia University).

[2]email: turnshek@quasar.phyast.pitt.edu, rao@everest.phyast.pitt.edu, dbn@phyast.pitt.edu, wlane@astro.rug.nl, monier@astronomy.ohio-state.edu, jbergero@eso.org, asmette@band3.gsfc.nasa.gov

[3]also Kapteyn Astronomical Institute, University of Groningen (present address).

[4]also Ohio State University (present address).

morphological structure. Assuming there is no contribution from the quasar host galaxy, we place an upper limit on the K-band luminosity of the $z = 0.09$ DLA galaxy of $L_K \leq 0.13L_K^*$ (assuming a cosmology with $H_0 = 65$ km s^{-1} Mpc^{-1}, $\Omega = 1$, and $\Lambda = 0$). More realistically, a subtraction of the quasar nuclear and host light yields $L_K \approx 0.08L_K^*$. The impact parameter between the galaxy and quasar sight-line is very small, $b < 3.6$ kpc (< 2 arcsec), which makes measurements difficult. The $z = 0.22$ DLA galaxy is an early-type dwarf with a K-band luminosity of $L_K \approx 0.1L_K^*$ at impact parameter $b = 20$ kpc. Its colors are neutral and consistent with star formation models suggesting its formation epoch was less than a few Gyr ago (i.e. $z_f \approx 0.3 - 0.9$). Thus, it is conceivable that its progenitor originated from the population of "faint blue galaxies" seen at moderate redshifts. In general, these results serve to support mounting evidence that DLA galaxies are drawn from a wide variety of gas-rich galaxy types.

Subject headings: quasars: absorption lines — quasars: individual (OI 363, 0738+313) — galaxy formation

1. INTRODUCTION

The $z_{abs} = 0.0912$ and $z_{abs} = 0.2212$ damped Lyα (DLA) absorption-line systems along the sight-line toward the quasar OI 363 (0738+313) have been the subject of several recent papers by members of our group. Rao & Turnshek (1998, hereafter RT98) announced the discovery of these systems during the course of an HST-FOS survey for DLA absorption in QSO MgII systems.[5] In this paper they discussed the results of a preliminary optical imaging search for galactic light from these two absorbers, and they concluded that the galactic counterparts are definitely not luminous spirals. Lane et al. (1998a,b) and Lane, Briggs & Smette (2000a) presented the results of 21 cm observations along the sight-line toward OI 363. They found that both of the damped systems exhibit 21 cm absorption. However, an initial search for 21 cm emission from the lower-redshift system failed to detect a signal (Lane et al. 2000b).

The existence of these two systems is noteworthy because they currently represent the two lowest-redshift classical quasar DLA absorption-line systems which are confirmed, i.e., actual UV spectroscopic observations of their DLA profiles exist and analyses of the spectra demonstrate that the systems' neutral hydrogen column densities are above the classical survey limit of $N_{HI} \geq 2 \times 10^{20}$ atoms cm^{-2}. In several other reported cases of low-redshift DLA systems, either confirming UV spectroscopy is lacking (Miller, Knezek & Bregman 1999), the H I column density is somewhat below the classical limit (Lanzetta et al. 1997), or both. Thus, although detection of foreground galaxies near a bright background QSO remains difficult, the OI 363 sight-line offers a most ideal opportunity for studying any emission from stellar and gaseous components of objects responsible for classical DLA absorbers. We refer to such luminous objects as DLA galaxies.

Here we report on the results of new observations of galaxies along the sight-line toward OI 363. The data consist of optical and infrared imaging and also optical spectroscopy in seeing conditions sometimes as good as ≈ 0.55 arcsec. Throughout the analysis we assume $H_o = 65$ km s^{-1} Mpc^{-1}, $\Omega = 1$, and $\Lambda = 0$; we also adopt the naming convention used in RT98. In §2 we start by summarizing the results from our earlier studies. In §3 the new observations and analyses of these data are presented. In brief, the DLA galaxy associated with the $z = 0.0912$ absorber appears to be an extended low surface brightness dwarf galaxy at impact parameter $b < 3$ kpc, with rich morphological structure and a K-band luminosity of $L_K \leq 0.08 - 0.13L_K^*$, where the measured light is an upper limit depending on the amount of contamination from the quasar host galaxy at redshift $z \approx 0.63$ ($L_K \leq 0.13L_K^*$

[5]The results of the full spectroscopic survey for low-redshift DLA systems are discussed in Rao & Turnshek (2000).

assumes no host contribution). The DLA galaxy associated with the $z = 0.2212$ absorber is considerably different in character; it is an early-type dwarf galaxy which is relatively compact at an impact parameter of $b = 20$ kpc, with a K-band luminosity of $L_K \approx 0.1 L_K^*$. In §4 we discuss the implications of these findings.

2. PREVIOUS RESULTS

RT98 presented the HST-FOS UV spectrum of OI 363 (see their figures 1-3) which led to the identification of the two absorbing systems at $z_{abs} = 0.0912$ and $z_{abs} = 0.2212$ with H I column densities of $N_{HI} = (1.5 \pm 0.2) \times 10^{21}$ atoms cm^{-2} and $N_{HI} = (7.9 \pm 1.4) \times 10^{20}$ atoms cm^{-2}, respectively.

RT98 also presented a 45 min R-band WIYN image of the OI 363 field in seeing of 0.55 arcsec (see their figure 4). Analysis of this image resulted in a list of 15 resolved objects and 11 point sources brighter than R = 24 mag within 40 arcsec of the quasar sight-line (see their table 1). The closest resolved object was found to be a galaxy (named G1, R = 20.8 mag) 5.7 arcsec to the south-southeast of the quasar and the closest unresolved object is presumably a star (named S1, R = 20.8 mag) 2.5 arcsec to the northeast of the quasar. Fainter objects were visible in the R-band WIYN image but they were not tabulated since such a list would have suffered from incompleteness. However, the existence of a marginally significant fainter extended feature a few arcsec to the west-southwest of the quasar sight-line was noted (marked with a cross on figure 4 of RT98). It appears to be the brightest part of the "fuzz" near the quasar, and was reported to have an R-band surface brightness of ≈ 25.3 mag arcsec^{-2}. Notably, the brightest galaxy in the field is a luminous spiral (named G11, R = 17.1 mag) ≈ 31 arcsec to the east of the quasar with a redshift of $z \approx 0.06$. A similarly luminous spiral at a somewhat larger redshift of $z = 0.09$, i.e., the redshift of the lowest redshift DLA absorber, could have easily been detected in this field if it was present, but the observations ruled this out. We note that there is an absorption line at ≈ 1290 Å in the original FOS low-resolution spectrum of the quasar, which can be identified as Lyα with a rest equivalent width of W≈ 0.7 Å and a redshift of $z_{abs} \approx 0.06$. The existence of a Lyα line at $z = 0.06$ is consistent with the results of Guillemin & Bergeron (1996). In any case, due to their close proximity to the quasar sight-line in comparison to other objects in the field, the galaxy labeled G1 and any object that might be associated with the fuzz are of most significant interest; the results from our new observations (§3) indeed suggest that these luminous objects can be identified with the two DLA galaxies.

Both of the DLA absorbers along this sight-line have been shown to have associated

H I 21cm absorption (Lane et al. 1998a,b and 2000a; Chengalur & Kanekar 1999). The $z_{abs} = 0.2212$ system shows only a single narrow 21 cm absorption feature, while the $z_{abs} = 0.0912$ system has complex velocity structure. The spectrum from this lower redshift system is best fit by multiple Gaussians: two narrow cold components with thermal kinetic widths of $T_k \approx 300$ and 100 K, and a third broad component with $T_k \approx 5000$ K (Lane et al. 2000a). This suggests the presence of two temperature phases for the neutral medium, similar to those found in the Galaxy. For this lower redshift system, excluding the velocity interval where absorption is detected (a region covering ≈ 55 km s^{-1}), an upper limit has been placed on the H I gas mass. Sensitive WSRT 21 cm emission measurements of the $z_{abs} = 0.0912$ absorber place the upper limit at $M_{HI} \leq 3.7 \times 10^9 h_{65}^{-2}$ M$_\odot$ for an assumed velocity spread of 100 km s^{-1} (Lane et al. 2000b). This requires the H I mass of the absorber to be somewhat less than that of a normal spiral galaxy. In principal, since the velocity spread would be lower for a more face-on spiral, the formal H I mass limit for this special case could be even lower. However, if the 21 cm emission were confined to a very narrow velocity interval, one might then be concerned that a significant amount of the 21 cm emission were missed because it fell in the same velocity intervals as the absorption.

3. OBSERVATIONS AND ANALYSES OF NEW DATA

New observations along the sight-line toward OI 363 include optical and infrared imaging and optical spectroscopy. Based on our identifications, here we exclusively consider analysis of the data pertaining to galaxy G1 and the fuzz near the quasar. G1 is shown to be a dwarf galaxy at redshift $z \approx 0.22$, consistent with the redshift of the $z_{abs} = 0.2212$ DLA absorber. We argue that at least part of the fuzz is associated with the $z_{abs} = 0.0912$ DLA absorber, leading to the interpretation that the $z = 0.09$ DLA galaxy is an extended low surface brightness dwarf galaxy with rich morphological structure.

3.1. Optical Imaging

Optical BRI imaging data of the OI 363 field were obtained for us by the WIYN Queue team using a 2048×2048 Tektronics STIS thinned, frontside illuminated CCD (0.195 arcsec per pixel) on the 3.5-m WIYN Telescope on Kitt Peak. In addition, we obtained supplemental U-band imaging data using the 1024×1024 Templeton thinned, backside illuminated CCD (0.28 arcsec per pixel) on the MDM Observatory 2.4-m Hiltner Telescope on Kitt Peak. The seeing ranged between $\approx 0.55 - 1.0$ arcsec. The journal of observations for these optical images is presented in Table 1. These data were processed using normal

methods. Observations of standard stars and field stars in the quasar frame allowed us to obtain calibrated magnitudes on the Johnson (U, B) and Cousins (R, I) system. We note that the R calibration is consistent with the calibration used in RT98 which was originally based on the calibration of Drinkwater, Webster, & Thomas (1993). However, the four color images are not shown here because they do not reveal any additional qualitative information beyond what can be learned from inspection of the R-band WIYN image that was published by RT98.

3.2. Infrared Imaging

Infrared imaging observations of the OI 363 field in JHK were obtained on the 3.0-m NASA IRTF on Mauna Kea using NSFCAM, a 256×256 InSb detector array (0.30 arcsec per pixel). The journal of observations for these infrared images is also presented in Table 1. The observations were obtained during the course of three different observing runs in various observing conditions. The conditions were not always photometric and there were variations in the infrared sky brightness; the seeing ranged between $0.75 - 1.0$ arcsec. Using recommended procedures (see the irtf.ifa.hawaii.edu/Facility/nsfcam/nsfcam.html WEB site), the observations were obtained using several different short-exposure dither patterns, flatfielded with sky frames that were obtained from the dithered object frames, and then shifted before addition to obtain a "final" image. Since several different standard stars were used and the data were collected on a variety of dates, this provided multiple opportunities to check the photometric calibrations. Panels (a) and (b) of Figure 1 show one of the K band images (60 min) of the OI 363 field and its associated isophotal plot. This was one of the best K-band images in the sense that it had good seeing (≈ 0.75 arcsec) and a low K-band sky brightness, allowing very low surface brightness features to be revealed. For display, this image was smoothed with a Gaussian (FWHM = 0.75 arcsec) and the unresolved nuclear PSF was then subtracted (see §3.4.2 for discussion of this process). Due to poorer seeing and/or higher background sky levels, the remaining K-band images provided little additional information, with the exception of the checks of the photometric calibration.

3.3. Optical Spectroscopy of G1

Optical spectroscopic observations of objects in the OI 363 field were obtained using the NOAO 4.0-m Mayall Telescope on Kitt Peak. The aim of the spectroscopy was to identify or exclude objects near the DLA redshifts of $z = 0.22$ and $z = 0.09$. We will only

present the spectrum of G1 here since the fuzz near the quasar was too faint to obtain a reliable spectrum and the other spectra we obtained did not result in identifications for either of these two redshifts.

Spectra of objects in this field were obtained with the CRYOCAM in long-slit and multi-slit modes. Since G1 is both faint and close to the bright QSO, obtaining its spectrum was difficult. We found that the long slits produced stronger object signals that were easier to measure relative to sky than the short multi-slit masks. The final spectrum of G1 is a combination of two long-slit spectra obtained separately with the Grism 650 (400 l mm^{-1} covering $4000 - 6800$ Å) and the Grism 770 (300 l mm^{-1} covering $4300 - 8500$ Å). The bluer spectrum was obtained in 120 minutes on the night of 29 April 1998 with a 1.7 arcsec wide slit at a resolution of ≈ 10 Å (3.2 Å per pixel); the redder spectrum was obtained in 90 minutes on the night of 14 Feb 1999 with a 1.0 arcsec wide slit at a resolution of ≈ 12 Å (4.3 Å per pixel). The slit width used was matched to the seeing conditions as closely as possible. Wavelength calibration of the spectra was accomplished with the observation of an internal HeNeAr lamp. The G1 spectra were extracted from the flatfielded Loral (Ford) CCD images after removal of cosmic rays using an optimal extraction algorithm. The spectra were initially flux-calibrated using standard star observations, adjusted to the same flux level in the overlapping region and combined by variance weighting. The observations produced a useful spectrum of G1 over the wavelength interval $4500 - 8500$ Å. The f_λ spectrum, rebinned to ≈ 12 Å pixels and normalized in flux at 6000 Å, is shown in Figure 2. The downturn in the flux beyond 8000 Å is possibly due to poor calibration at the red end of the Grism 770 spectrum where the spectrograph becomes more defocussed.

3.4. The Properties of Two Low-Redshift DLA Galaxies

The IRTF K-band image (Figure 1) shows G1 (≈ 5.7 arcsec southeast of the quasar) and reveals the presence of luminous features in the fuzz surrounding the quasar that were not very significant in the RT98 WIYN R-band image. The fuzz is seen to consist of features of low, but not uniform, surface brightness. One gets the impression that, within the fuzz, the elongated feature to the east-southeast of the quasar could be part of a (spiral) "arm" since it is approximately concentric with respect to the somewhat off-centered light surrounding the quasar; a similar arm is not apparent on the opposite side of the quasar. To the west-southwest there is a feature elongated from east to west that appears like a "jet" since it runs nearly perpendicular to the otherwise concentric-looking extended light. This jet-like feature appears to have structure. It is coincident with the cross marked on the original RT98 WIYN R-band image, but it does not emanate from the quasar nucleus.

In the discussion below we will use the terms "arm" and "jet" to describe the appearance of these features, but there is certainly no *strong* evidence that these terms describe their actual physical nature.

Table 2 lists the UBRIJHK photometric measurements of G1, the arm, and the jet. Details of how these measurements were made and how they have been used to infer the properties of the two DLA galaxies at $z = 0.22$ and $z = 0.09$ are given below. Since we have a spectrum of G1, we will consider it first.

3.4.1. G1 ($z = 0.22$)

3.4.1.1. The Spectrum

The spectrum of G1 is shown in Figure 2. For comparison, the spectrum of an early-type galaxy (the type E3 elliptical galaxy NGC 4648, Kennicutt 1992a), redshifted to $z = 0.22$ and normalized at 6000 Å, is also plotted. This template spectrum is offset relative to the spectrum of G1 for clarity. The spectrum of this early-type galaxy template over our observed wavelength range is dominated by the spectral features of cool giants, i.e., the 4000 Å break, the G band at rest wavelength 4304 Å, the MgI + MgH (Mgb) band at 5175 Å, the NaD lines at 5893 Å, and a TiO band at 6260 Å. The positions of these features as they appear in the redshifted spectrum of NGC 4648 are marked. The telluric B band in this spectrum also appears redshifted, since it was not removed from the original Kennicutt (1992a) spectrum. The unredshifted telluric A and B bands as they appear in the spectrum of G1 are also marked.

We see from its spectrum that G1 is probably best classified as a dwarf elliptical, or possibly E/S0. The two most prominent features in the spectrum of G1 that suggest it is at redshift $z \approx 0.22$ are the 4000 Å break and the absorption feature that corresponds to the position of the MgI+MgH band. The narrow downward spike within this Mg band is caused by residuals from subtracting the 6300 Å night sky line. The shape of the continuum between 4500 Å and 8000 Å matches the E-type galaxy template spectrum remarkably well. However, given the spectrograph slit size, which corresponds to ≈ 5 kpc in the blue and ≈ 3 kpc in the red for $z = 0.22$, a reasonable interpretation would also be that the light being sampled by the spectrograph originates in the *bulge* of an early type spiral galaxy. Template spectra of early type spirals (S0 and S0/a) with non-Seyfert nuclei (Kennicutt 1992a) also show the same characteristic continuum shape and spectral features as the E galaxy spectrum shown on Figure 2. Emission lines, in particular Hα, are weak in the integrated spectra of Sa galaxies and are not present in earlier types, so the absence of Hα and other emission lines in the spectrum of G1 also strongly indicates that G1 is an early type galaxy.

The expected position of Hα at $z = 0.22$ is marked on Figure 2. Kennicutt (1992b) points out that the equivalent width of [OII]λ3727 emission in galaxies is typically one-third that of Hα, so the absence of [OII] (which is in the most noisy part of the spectrum) is consistent with the absence of Hα; moreover, when Hα is weak (as is the case here) the equivalent width of [OIII]λ5007 rarely exceeds $\approx 1 - 2$ Å, so it would also not be expected.

It is interesting that some dwarf Es, E/S0s, and S0s are known to have substantial H I halos (e.g. Lake, Schommer & van Gorkom 1987 and Sadler et al. 2000), extending up to $\approx$ 5 times the optical radius. The H I column densities in the inner contours easily exceed the $2{\times}10^{20}$ atoms cm^{-2} requirement for producing a classical DLA absorption line. Unlike the luminous Es and S0s, these early-type dwarf galaxies are H I-rich for their morphological class, with centrally concentrated neutral gas and H I masses of a few times $10^8 - 10^9$ M$_\odot$. However, these early-type H I-rich dwarfs are evidently rare locally.

The apparent magnitude and spectrum of G1 is reminiscent of some of the faintest galaxies discovered in the Hawaii K-band survey of Songaila et al. (1994, e.g., see their object number 265 in field SSA22). Indeed, examination of the statistical results on the Hawaii deep survey fields presented by Cowie et al. (1996) indicates that G1 is intrinsically one of the faintest galaxies near redshift $z \approx 0.22$ in comparison to their sample.

We note that the spectrum of G1 recently obtained by Cohen (2000) is consistent with our interpretation.

3.4.1.2. The Spectral Energy Distribution

Since our imaging data were taken with three different telescopes in various conditions and with widely varying limiting magnitudes, an appropriate procedure had to be used to accurately determine G1's colors. The worst seeing conditions ($\approx$ 1.0 arcsec) were in the U and H bands. Therefore, all of the other images (BRIJK) were degraded to this resolution by convolution with a Gaussian before the photometric measurements were made. An aperture size of 1.4 arcsec ($\approx$ 4.9 kpc at $z = 0.22$) was then determined to be a good choice to include most of the galactic light detectable above the sky background in the faintest image and still yield minimal errors. However, we note that nearly half of G1's light in the WIYN R-band was not included in the 1.4 arcsec aperture using this method. Extrapolation was then used to derive total magnitudes. Comparison of the WIYN B-band and R-band images, which represents our best two-color data, showed no *significant* evidence for a color gradient in G1. The estimated errors in G1's magnitudes (Table 2) include both the statistical errors and zero-point calibration errors.

We see that G1 is a neutral-colored dwarf galaxy (B$-$K= 4.9) with $L_K = 0.10L^*_K$, $L_R = 0.12L^*_R$ and $L_B = 0.10L^*_B$, where an L^* galaxy corresponds to $M^*_K = -24.5$,

$M_R^* = -21.9$ and $M_B^* = -20.9$ (see Loveday 2000 for M_K^*, Marinoni et al. 2000 for M_B^*, and Poggianti 1997 and Cowie et al. 1994 for K corrections).

Given the UBRIJHK colors of G1, we point out that further evidence of its redshift comes from a derivation of its photometric redshift. As Figure 3 shows, $z = 0.2$ is the most probable redshift based on fitting 1996 Bruzual and Charlot galaxy model templates to the colors (see more discussion below). In particular, it was possible to obtain an excellent match to the spectral energy distribution of G1 using a spectral synthesis code to model a galaxy near redshift $z = 0.22$. While we considered a variety of metal abundances, the fits were not very sensitive to metallicity for these colors. However, slightly higher and lower redshifts could not be ruled out definitively based on the photometry alone (Figure 3) and, in the end, the best evidence for the $z = 0.22$ redshift of G1 comes from its slit spectrum (Figure 2) and the circumstantial evidence provided by the existence of the $z = 0.2212$ absorber in the field. Therefore, while the derivation of photometric redshifts for intrinsically faint DLA galaxies would seem to be a promising method when used with the expectation that there will be a galaxy in the field at the absorption redshift, the technique should be used with caution since most photometric redshift techniques have been tested by comparing photometric and spectroscopic redshifts of intrinsically luminous galaxies, but evidence (§4) suggests that DLA galaxies are often not very luminous.

In order to consider how well the observed colors of G1 at $z = 0.22$ match different types of galaxies, and what this might tell us about the present nature of G1 and its progenitor, we used the publicly available photometric redshift code *hyperz* (Bolzonella, Pello & Miralles 2000) to produce spectral synthesis models. First we dereddened the colors of G1 using a Galactic extinction law and $A_B = 0.18$ (Cardelli, Clayton, & Mathis 1989). We then used *hyperz* to investigate the range of models and ages that produced acceptable fits to the observed colors of G1. For our analysis we set the metallicity to 20% of the solar value. The amount of intrinsic visual extinction, A_V, was allowed to be a free parameter, assuming that the Calzetti et al. (2000) reddening law holds. The available GISSEL96 template sets were for an instantaneous single-burst model, plus models with exponentially decreasing star formation rates with e-folding times in Gyrs of $\tau = 1$, 2, 3, 5, 15, 30, and infinity (i.e. constant star formation rate). Models with $\tau < 3$ are generally taken to correspond to early type galaxies (e.g. type E or S0). Of these models, the burst models at ages between $0.36 - 3.5$ Gyrs, and with A_V ranging between $1.3 - 0.1$, respectively, were found to give acceptable fits to the color data. Also, a $\tau = 1$ model with $A_V = 0.5$ fits the color data reasonably well at an age of 3.5 Gyrs. A 0.72 Gyr old burst model with $A_V = 1.1$ mag gave the best overall fit. [We note that for the Cardelli et al. (1989) Galactic extinction law, $A_V = 1$ corresponds to $N_{HI} = 1.9 \times 10^{21}$ atoms cm^{-2}; while for the Calzetti et al. (2000) extinction law which we used in the *hyperz* simulations, $A_V = 1$ might lie in the

range $N_{HI} = 0.4 - 2.0 \times 10^{21}$ atoms cm^{-2}, but a good estimate is hindered by the absence of a metallicity measurement for G1. This should be compared to the value observed in the $z = 0.22$ absorber at impact parameter $b = 20$ kpc, $N_{HI} = 1.5 \times 10^{21}$ atoms cm^{-2}.] Figure 4 shows the color data with the models over-plotted. The best-fitting model is in panel (a) and three reasonable alternative models are shown in panels (b), (c), and (d). These galaxy templates are generally consistent with the observed spectrum of G1 (Figure 2). A comparison of the model fits shown in Figure 4 indicates that far-UV observations could break some of the UBRIJHK color degeneracy which makes it hard to distinguish age and extinction in burst models. Thus, lacking far-UV photometry of G1, we can only infer that the progenitor population originated at a formation epoch between $z_f \approx 0.26$ (corresponding to the 0.36 Gyr old burst model) and $z_f \approx 0.84$ (corresponding to the 3.5 Gyr old models). For the four models illustrated in Figure 4, we show in Figure 5 the corresponding inferred color (B−K) evolutionary history of G1's progenitor prior to its current state at $z = 0.22$, including effects due to the K-correction but assuming that no change in intrinsic dust extinction occurred. As would be expected, in all cases the color evolution suggests that the progenitor of G1, with B−K= 4.9 at $z = 0.22$, would have been considerably bluer close to its formation epoch, i.e., B−K<4 at $z \approx z_f$. Therefore, we conclude that G1 might be a faded, low-redshift counterpart originating from the population of moderate-redshift ($z \approx 0.3 - 0.9$) "faint blue galaxies" that have been identified in surveys (e.g. Ellis 1997 and references therein). Further details are given in the next section.

3.4.1.3. The Star Formation Rate

An upper limit to the Hα flux in the spectrum of G1 (Figure 2) has been estimated. This was done by first correcting the continuum shape near 8000 Å to match that of the Figure 2 comparison spectrum. The absolute flux zero point was then obtained by adjusting this corrected, standard-star-calibrated spectrum by a constant scaling factor to make it agree with the more accurate optical photometric measurements. Measurement of the spectrum using a slit corresponding to a width of ≈ 3 kpc near Hα yields a 4σ upper limit on the rest frame Hα flux of $f_{H\alpha} < 2.5 \times 10^{-16}$ ergs cm^{-2} s^{-1}, as measured over an ≈ 12 Å interval. At $z = 0.22$ this translates to an Hα luminosity of $L_{H\alpha} < 3.4 \times 10^{40}$ ergs s^{-1} and a corresponding star formation rate < 0.3 M$_\odot$ yr^{-1} (Kennicutt 1992b). This limit is not unexpected for the bulge-dominated region of a galaxy.

We can also specify the details of the star formation process that correspond to the spectral synthesis models which were discussed in the previous section and illustrated in Figures 4 and 5. Using the total magnitudes given in Table 2 we find that: (a) for the best-fitting 0.72 Gyr old burst model there is (of course) no current star formation and the total stellar mass involved is 5.8×10^9 M$_\odot$, (b) for the 0.36 Gyr old burst model the total

mass is 5.3×10^9 $M_\odot$, (c) for the 3.5 Gyr old burst model the total mass is 7.1×10^9 $M_\odot$, and (d) for the 3.5 Gyr old $\tau = 1$ model the total mass is 7.6×10^9 $M_\odot$, where the initial star formation rate is 7.8 $M_\odot$ yr^{-1} and the star formation rate at $z = 0.22$ is 0.24 $M_\odot$ yr^{-1}. This is consistent with our upper limit on the star formation of 0.3 $M_\odot$ yr^{-1} from Hα. We note that using total magnitudes (Table 1) results in stellar masses and star formation rates that are about a factor of two larger than when aperture magnitudes are used.

3.4.1.4. The Radial Brightness Profile

The radial brightness profile of G1 is also of interest. Using the WIYN R-band data with the best seeing ($\approx$ 0.55 arcsec), we analyzed the radial brightness profile of G1. The observed light profile is the convolution of the true, two-dimensional light profile and the image point-spread function. If the true profile is symmetric and the PSF is well approximated by a Gaussian, the convolution reduces to a simple one-dimensional integral (see Binney & Tremain 1987) that makes it possible to compare a model radial brightness profile to the data in a straightforward manner. The observed light profile of G1 is very close to symmetric, so we used this method. Elliptical isophotes were fitted to the brightness profile of G1. The resulting radial brightness profile along the semi-major axis is shown in Figure 6. Three models were fitted to the data: (a) a pure $r^{1/4}$ (bulge) profile, (b) a pure exponential (disk) profile, and (c) a combination bulge-disk profile. As shown in the corresponding panels (a-c) of Figure 6, a pure-disk model is a poor fit, while a pure-bulge model gives better results. The bulge-disk combination is clearly the best fit and is the preferred model, but it includes an extra free parameter. This simple model and the small angular extent of G1 compared to the seeing make it difficult to pin down the bulge-to-total light ratio, the bulge half-light radius or the disk scale-length with accuracy, but our fits suggest that a moderate amount of each is necessary to fit the light profile well.

Owing to the need for some disk light, this result therefore seems reasonably consistent with the interpretation that G1 is an early-type "dwarf spiral," which has been discussed as a recently-recognized new class of galaxy (Schombert et al. 1995). In many respects these galaxies resemble the H I-rich dwarf Es, E/S0s, and S0s mentioned in §3.4.1.1. According to Schombert et al., the dwarf spirals are found only in the field and have total luminosities $M_B > -17.6$, diameters $R_{26} < 6.5$ kpc, low central surface brightnesses $\mu_0 > 24$ B mag arcsec^{-2}, and low H I masses $M_{HI} \leq 1.7 \times 10^9$ $M_\odot$ (converting the Schombert et al. values to our assumed cosmology with $H_0 = 65$ km s^{-1} Mpc^{-1}). This represents a class of objects which are currently rich in neutral gas, small in angular size, and low in surface brightness. The central surface brightness of G1 ($\mu_0 \approx 23.4$ B mag arcsec^{-2}) is somewhat brighter than the parameters given by Schombert et al.

3.4.1.5. The H I Mass Estimate

G1 is displaced 5.7 arcsec from the quasar sight-line, corresponding to an impact parameter of $b = 20$ kpc. This is a relatively large impact parameter in relation to the apparent optical size of G1 (Figure 1). It is not unusual to find evidence for a relatively large impact parameter when trying to identify galaxies giving rise to quasar absorption-line systems, but it is somewhat surprising for a DLA system and so it leaves open the possibility that the site of the absorption is an H I cloud in a galaxy that is a companion to G1. However, consideration of this is beyond the scope of the available data, so we have only concentrated on the description of G1 here. We note that if the $z = 0.2212$ absorber is assumed to have a uniform H I column density of $\approx 7 \times 10^{20}$ atoms cm^{-2} and extend over a radius equal to the impact parameter, then its deduced H I mass is $M_{HI} \approx 2.8 \times 10^{10}$ $M_\odot$. This H I mass estimate is about an order of magnitude greater than quoted above for H I-rich dwarf Es, E/S0s, S0s, or spirals.

3.4.2. The "Fuzz" Near the Quasar ($z = 0.09$)

The arm and jet are the two brightest patches of low surface brightness extended light near the quasar (i.e. the "fuzz"). Since we do not have a useful spectrum of any part of the fuzz, or data that can be used to derive a photometric redshift for these features, their redshifts cannot be known with certainty. In principal, the light could be from a combination of: (1) unrelated foreground or background objects at neither of the two damped redshifts, (2) the quasar host galaxy at $z = 0.63$, (3) the "true" DLA galaxy at $z = 0.22$ (assuming that G1 at redshift $z = 0.22$ does not have a sufficient H I extent), and (4) the DLA galaxy at $z = 0.09$. Examination of the infrared images do suggest a combination of objects or perhaps a single disturbed object (see Figure 1). Therefore, we will discuss each of these four possibilities.

(1) Contamination from unrelated objects is possible. However, examination of the infrared images suggests that $< 1\%$ of the frame contains detectable infrared sources at the sensitivity of the K-band images. Therefore, if an unrelated object or objects are present near the quasar sight-line, this is an unlucky configuration, so we will not consider this possibility further.

(2) There is a reasonable chance that some of the quasar's host galaxy light at $z = 0.63$ is present in the infrared light surrounding the quasar. The quasar, OI 363, is optically luminous (V≈16.1, $M_V \approx -26.1$) and radio loud. Infrared studies of optically luminous, radio loud quasars in the H-band (McLeod & Reike 1994) show that it is not unusual for these types of quasars to have luminous host galaxies, e.g., $> 2L^*_H$, and HST-WFPC2 studies at $z < 0.46$ show that the host galaxies of radio loud quasars are almost exclusively

ellipticals (Hamilton, Casertano, & Turnshek 2000). Examination of the infrared OI 363 images after subtraction of the unresolved nuclear quasar light (Figure 1) indicates that the remaining light is not exclusively from an elliptical host centered on the quasar. A reasonable deconvolution of the image suggests that the nuclear quasar component has $M_K \approx -28.6$ ($L_K \approx 44L_K^*$) while its host has an $r^{1/4}$ profile and $M_K \approx -25.8$ ($L_K \approx 3.3L_K^*$), which is completely consistent with previous findings on radio loud quasar hosts. Nevertheless, after subtraction of the nuclear and host components some light remains between the arm and the jet. In any case, the mere presence of the arm and the jet indicates that the surrounding light is not exclusively associated with an elliptical host. An illustration of the light that we believe is dominated by the quasar elliptical host is contained within the ellipse drawn on Figure 1a. However, there are uncertainties with this deconvolution and better spatial resolution would be needed to accurately separate out the various components.

(3) The possibility that some of the extended, low surface brightness light surrounding the quasar is due to the DLA galaxy at $z = 0.22$ is dismissed since G1 is identified as the DLA galaxy. However, recall that the impact parameter of G1 is 5.7 arcsec or $b = 20$ kpc, which may be large for a dwarf galaxy giving rise to DLA absorption (§3.4.1.5).

(4) From the arguments presented above (1-3), we conclude that *some* of the light surrounding the quasar is from the DLA galaxy at $z = 0.09$.

Owing to the approximately circular nature of the resolved light, regardless of whether a contribution from an elliptical host is removed, and the possibility of an actual spiral arm, it may be that this DLA galaxy is a nearly face-on spiral. If this turns out to be the case, the low surface brightness dwarf spiral interpretation might in fact be more descriptive of the $z = 0.09$ DLA galaxy than for G1 at $z = 0.22$ (§3.4.1.4). At the same time, the considerable morphological structure surrounding the quasar leaves open the possibility that the $z = 0.09$ DLA galaxy is an irregular or an interacting system. In any case, if we want to place a conservative *upper limit* on the light from the $z = 0.09$ DLA galaxy it is appropriate to assume that *all* of the light surrounding the unresolved part of the quasar image (including what we believe to be the quasar host) belongs to it. With this assumption we obtain an upper limit on the K-band luminosity of the DLA galaxy at $z = 0.09$ of $L_K \approx 0.13L_K^*$. Assuming the arm and jet are both at $z = 0.09$, the arm has $L_K \approx 0.0007L_K^*$ with color R−K>5.5 (i.e. it is red and not detected in our R-band WIYN data) and the jet has $L_K \approx 0.0005L_K^*$ with a blue color of R−K≈3.2. This would imply that the jet is a site of relatively recent star formation, while the arm is an older population. We estimate the diameter of the measurable light distribution to be $\approx 7 - 9$ arcsec, or $\approx 12 - 16$ kpc, and the separation from the quasar sight-line to be < 2 arcsec, or impact parameter $b < 3.6$

kpc. As noted above, light contributed by an elliptical quasar host galaxy (i.e. some light inside the ellipse shown on Figure 1a) might have to be subtracted from the measured upper limit on the DLA galaxy's light in order to determine its true luminosity. In fact, a reasonable deconvolution suggests that the quasar host contributes $\approx 50\%$ of the total measured light, in which case the luminosity of the $z = 0.09$ DLA galaxy is $L_K \approx 0.08 L_K^*$. Regardless of the amount of contribution from the host galaxy, the resulting interpretation is that the $z = 0.09$ DLA galaxy is a low surface brightness galaxy with a diameter of ≈ 14 kpc at low impact parameter from the quasar sight-line. The details cannot be sorted out definitively without better data. Thus, the morphology of this low surface brightness dwarf galaxy remains uncertain − (another?) dwarf (possibly face-on) spiral, or an irregular, or an interacting system.

Given the above indication of the putative $z = 0.09$ DLA galaxy's diameter, it is useful to estimate its H I gas mass using some reasonable assumptions. If we simply assume that the circular H I gas radius is the same as the extent of the galaxy seen in the K-band image (i.e. radius r ≈ 7 kpc) and that the H I column density is uniformly $N_{HI} \approx 1.5 \times 10^{21}$ atoms cm^{-2} over that extent, the deduced H I mass is $M_{HI} \approx 6.5 \times 10^9$ M$_\odot$. This is a factor of 2 larger than the upper limit of Lane et al. (2000b) but, as discussed in §2.1, some of the H I 21 cm emission searched for by Lane et al. (2000b) may have been missed since velocity intervals which included absorption had to be excluded in their analysis. At the same time, the assumptions used above may over-estimate the H I mass since the impact parameter is evidently small and the H I gas distribution may be patchy or fall off exponentially with impact parameter. Nevertheless, the order of magnitude of this estimate is of interest; the total H I mass is smaller than our estimate for the $z = 0.2212$ DLA system (§3.4.1.5).

4. DISCUSSION

Although there are still open questions which better data could address, the findings discussed here represent some of the first results on the *detailed properties* of DLA galaxies. Perhaps fittingly, these results were determined from the two lowest redshift ($z = 0.09$ and 0.22) confirmed classical DLA systems known.

The results of our analysis indicate the following. The $z = 0.22$ DLA galaxy is a faint (B= 22.7, K= 17.8) neutral-colored (B−K= 4.9) dwarf galaxy with K- and B-band luminosities of $L_K = 0.10 L_K^*$ and $L_B = 0.10 L_B^*$, respectively. Its spectrum is that of an early type galaxy (S0 or even E). Analysis of the 7-color (UBRIJHK) data suggests that G1's spectral energy distribution is well-fitted by an instantaneous single-burst model with the burst taking place 0.36 ($A_V = 1.3$) to 3.5 ($A_V = 0.1$) Gyrs ago, or a 3.5 Gyr old model

with an exponentially decreasing star formation rate ($\tau = 1$ Gyr) and $A_V = 0.5$. Its current rate of star formation is low, < 0.3 $M_\odot$ yr^{-1}. Examination of the evolutionary history of these models leads us to conclude that the progenitor population of G1, if seen near the population's formation epoch at $z_f \approx 0.3 - 0.9$, would have properties similar to the population of "faint blue galaxies" presently observed at moderate redshift. Analysis of the extended radial light profile from the WIYN R-band image of G1 indicates that its outer isophotes are better fit by an exponential than an $r^{1/4}$ law, which offers some evidence for an early-type dwarf S0 or spiral interpretation. The putative $z = 0.09$ DLA galaxy is likely to be all or part of the resolved light surrounding the quasar. It is also a dwarf galaxy, and is inferred to have $L_K \leq (0.08 - 0.13)L_K^*$, with the higher value holding for the case where the quasar host galaxy at $z = 0.63$ does not contribute to the detected resolved light. There is considerable morphological structure in the light surrounding the quasar, including what we have called an arm and a jet. The arm is red in color and if it is an *actual* arm, this suggests that the DLA galaxy might be a low surface brightness dwarf spiral, but the presence of the other structure (i.e. a blue colored jet with apparent structure) leaves open the possibility that the DLA galaxy is an irregular or an interacting system. In any case, the $z = 0.22$ DLA galaxy is more compact, while the inferred DLA galaxy at $z = 0.09$ has low surface brightness. For these galaxies the H I gas masses deduced from the observed impact parameters and H I column densities lie in the range $M_{HI} \approx (6 - 23) \times 10^9$ $M_\odot$. These estimates are crude because we do not know if the observed H I is distributed like a face-on circular slab around the center of the identified DLA galaxy (like our calculation of the H I mass assumed) or whether the H I gas is exponentially distributed or clumped in giant clouds associated with the identified galaxy.

In any case, it would clearly have been much more difficult to deduce these properties from similar observations if these same objects were at moderate to high redshift. However, a collection of such detailed results, used in conjunction with statistical results on the incidence, cosmological H I gas mass density and column density distribution of DLA absorption systems (Rao & Turnshek 2000), will eventually be needed to accurately reveal the evolution of the bulk of the neutral gas in the Universe (as tracked by DLA quasar absorption systems) and the corresponding evolutionary relationship to DLA galaxies (i.e. the associated stellar light). One qualitative question presently of interest is to determine if the DLA population is slowly evolving from $z \approx 4.0$ to $z \approx 0.5$, as has been recently suggested by Pettini et al. (1999) and Rao & Turnshek (2000) on the basis of their metallicities and statistics, respectively. It would seem that there has to be some significant evolution in the DLA population from high to low redshift if the results of Rao & Briggs (1993) at $z = 0$ are correct. The Rao & Briggs (1993) study places almost all of the local H I gas in luminous spirals. Present evidence suggests that luminous galaxies

were approximately in place by $z \approx 1$, with less luminous galaxies showing more evolution at lower redshift (e.g. Im et al. 1996, 1999). Therefore, one could envisage a scenario where luminous galaxies contribute little to the DLA detections, except locally, while an evolving population of dwarfs and low surface brightness galaxies cause the bulk of the detections at $z > 0$. Indeed, the present searches for low-redshift DLA galaxies (Le Brun et al 1997; Turnshek et al. 2000) suggest that a significant fraction of them are dwarf and low surface brightness galaxies, and the possible connection to the evolving moderate redshift "faint blue galaxy" population mentioned earlier is intriguing. Clearly the statistical survey results and the low-redshift follow-up studies of DLA systems need to be extended and improved to address these evolutionary issues properly. It is also of interest to consider selection effects more carefully as well as design experiments which will reach to lower H I masses in searches for large quantities of H I gas not associated with luminous spirals. The current 21 cm emission surveys are sensitive to $M_{HI} \approx 10^7$ $M_\odot$ locally.

Regardless of the outcome of such new programs, the results reported here are consistent with our earlier findings (RT98) and serve to emphasize that DLA absorbing galaxies are not exclusively luminous spirals. They are drawn from a wide variety of types of gas-rich galaxies.

Acknowledgements

We wish to thank Dr. Frank Briggs for collaboration on parts of this program and Drs. Bolzonella, Pello, and Miralles for making their spectral synthesis code *hyperz* publicly available. We wish to also thank the support astronomers at the IRTF, Mayall, MDM, and WIYN telescopes for their assistance. This work was supported in part by an NSF grant and a NASA-LTSA grant.

REFERENCES

Bolzonella, M., Pello, R., & Miralles, J. 2000, A&A, in press (astro-ph/0003380)

Calzetti, D., Armus, L., Bohlin, R., Kinney, A., Koornneef, J., & Storchi-Bergmann, T. 2000, ApJ, 533, 682

Binney, J., & Tremain, S. 1987, in *Galactic Dynamics*, Princeton University Press

Bruzual, A., & Charlot, S. 1993, ApJ, 405, 538

Cardelli, J., Clayton, G., & Mathis, J. 1989, ApJ, 345, 245

Chengalur, J., & Kanekar, N. 1999, MNRAS, 302, L29

Cohen, J. 2000, astro-ph

Cowie, L., Songaila, A., Hu, E., & Cohen, J. 1996, AJ, 112, 839

Cowie, L., Gardner, J., Hu, E., Songaila, A., Hodapp, K., & Wainscoat, R. 1994, ApJ, 434, 114

Drinkwater, M., Webster, R., & Thomas, P. 1993, AJ, 106, 848

Ellis, R. S. 1997, ARA&A, 35, 389

Guillemin, P., & Bergeron, J. 1997, A&A, 328, 499

Hamilton, T., Casertano, S., & Turnshek, D. A. 2000, astro-ph

Im, M., Griffiths, R., Ratnatunga, K., & Sarajedini, V. 1996, ApJ, 461, 79

Im, M., Griffiths, R., Naim, A., Ratnatunga, K., Roche, N., Green, R., Sarajedini, V. 1999, ApJ, 510, 821

Kennicutt, R. 1992a, ApJS, 79, 255

Kennicutt, R. 1992b, ApJ, 388, 310

Lake, G., Schommer, R., & van Gorkom, J. 1987, ApJ, 314, 57

Lane, W., Smette, A., Rao, S. M., Briggs, F., Turnshek, D. A., & Meylan, G. 1998a, AJ, 116, 26

Lane, W., Briggs, F. H., Turnshek, D. A., & Rao, S. M. 1998b, BAAS, 193, No. 04.09

Lane, W., Briggs, F., & Smette, A., 2000a, ApJ, 532, 146

Lane, W., Briggs, F., Chengalur, J., & Kanekar, N., 2000b, in preparation

Lanzetta, K., et al. 1999, AJ, 114, 1337

Le Brun, V., Bergeron, J., Boisse, P., & Deharveng, J. 1997, A&A, 321, 733

McLeod, K., & Reike, G. 1994, ApJ, 420, 58

Miller, E., Knezek, P., & Bregman, J. 1999, ApJ, 510, L95

Pettini, M., Ellison, S., Steidel, C., & Bowen, D. 1999, ApJ, 510, 576

Poggianti, B. 1997, A&AS, 122, 399

Rao, S. M., & Briggs, F. H. 1993, ApJ, 419, 515

Rao, S. M., & Turnshek, D. A. 1998, ApJ, 500, L115 (RT98)

Rao, S. M., & Turnshek, D. A. 2000, ApJS, in press (astro-ph/9909164)

Sadler, E., Oosterloo, T., Morganti, R., & Karakas, A. AJ, 119, 1180

Scalo, J. 1986, in *Fundamentals of Cosmic Physics*, 11, p1

Songaila, A., Cowie, L., Hu, E., & Gardner, J. 1994, ApJS, 94, 461

Turnshek, D. A., Rao, S., Lane, W., Monier, E., Nestor, D., Bergeron, J., & Smette, A. 2000, to appear in *Gas & Galaxy Evolution*, ASP Conference Series, eds. J. Hibbard, M. Rupen, and J. van Gorkom, in press (astro-ph/0009096)

This preprint was prepared with the AAS LaTeX macros v4.0.

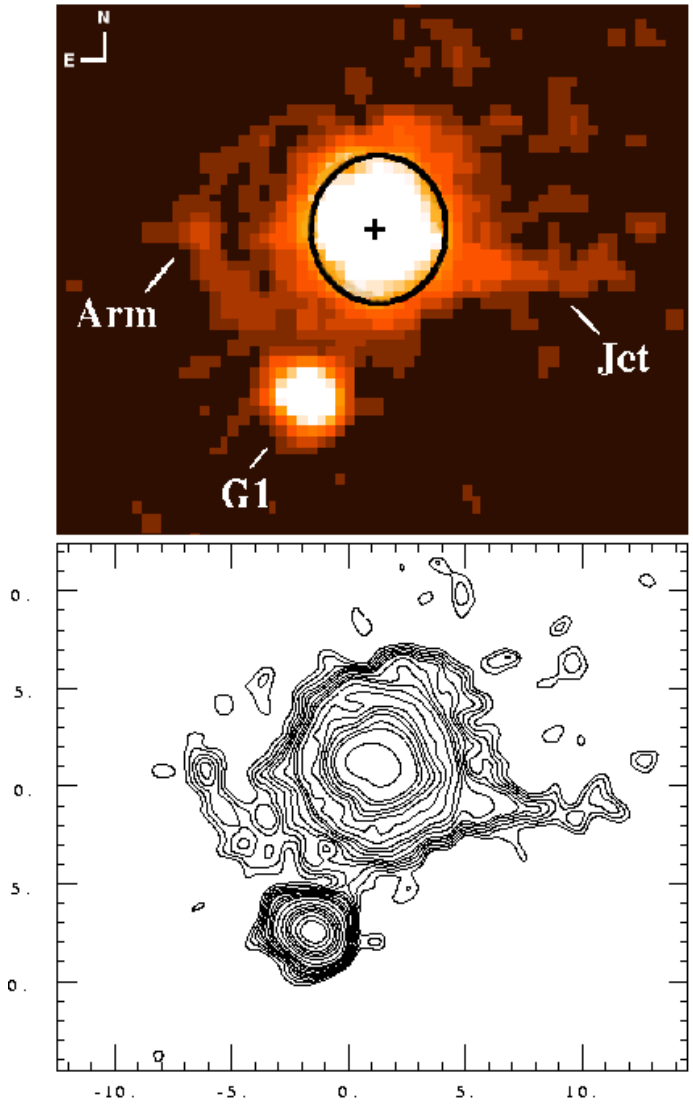

Fig. 1.— The top panel shows an IRTF K-band image of the OI 363 quasar field after smoothing with a Gaussian having a FWHM equivalent to the seeing (0.75 arcsec) and then subtracting the quasar's nuclear PSF. The center of the subtracted nuclear PSF is marked with a "+." The image is 20 × 17 arcsec. In the central region, enclosed in the ellipse drawn on the figure, the light appears to be dominated by an elliptical host ($M_K \approx -25.8$ or $L_K \approx 3.3L_K^*$ at $z_{Q,host} = 0.63$) to the quasar ($M_K \approx -28.6$ or $L_K \approx 44L_K^*$ at $z_{Q,nuc} = 0.63$). One or more of the low surface brightness features labeled "arm" and "jet", and the light between them (see text) is presumably due to the DLA galaxy at $z = 0.09$, corresponding to the DLA absorption-line system at $z = 0.0912$ with $N_{HI} = 1.5 \times 10^{21}$ atoms cm^{-2}. The dwarf galaxy labeled G1 is at $z = 0.22$, corresponding to the DLA absorption-line system at $z = 0.2212$ with $N_{HI} = 7.9 \times 10^{20}$ atoms cm^{-2}. The bottom panel shows an isophotal plot of the same region where the faintest isophote corresponds to 3σ above the background.

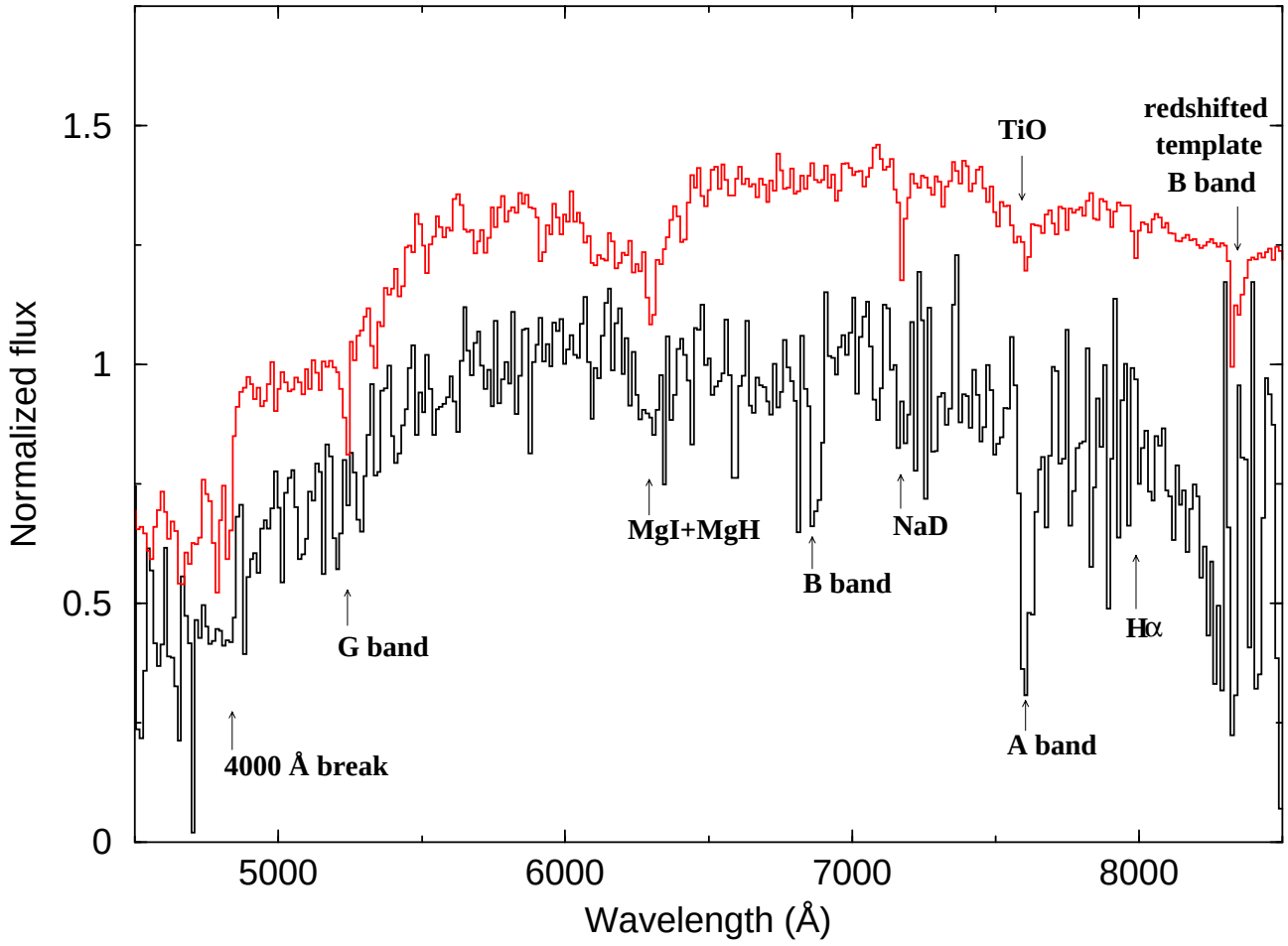

Fig. 2.— NOAO KPNO 4-m CRYOCAM spectrum of G1 with matching early-type galaxy template spectrum at $z = 0.22$ over-plotted. See §3.4.1.1 for a discussion of the spectrum.

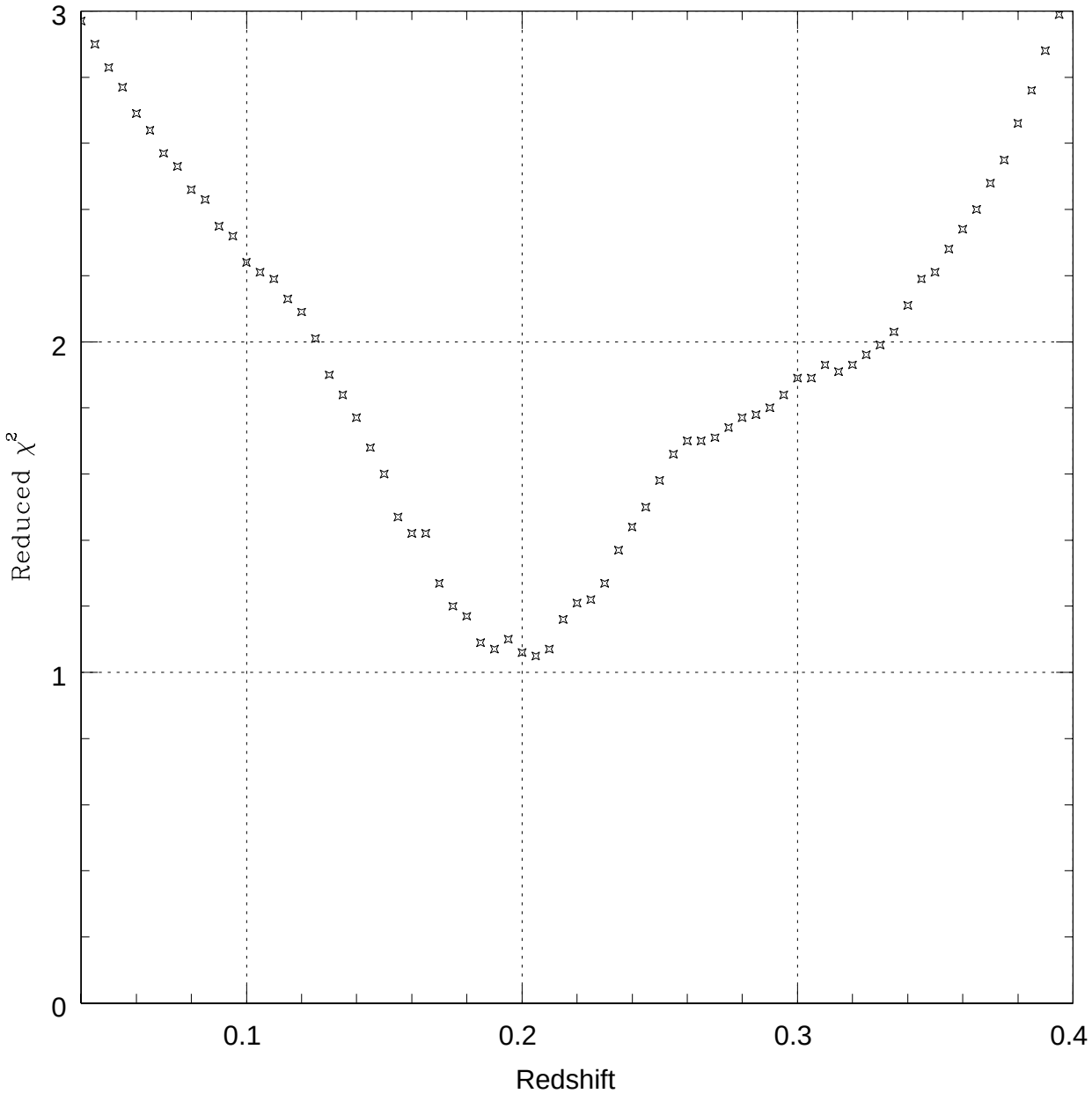

Fig. 3.— χ^2 plot showing the reliability of the photometric redshift determination for G1. The most probable photometric redshift is $z \approx 0.2$, which matches the slit redshift.

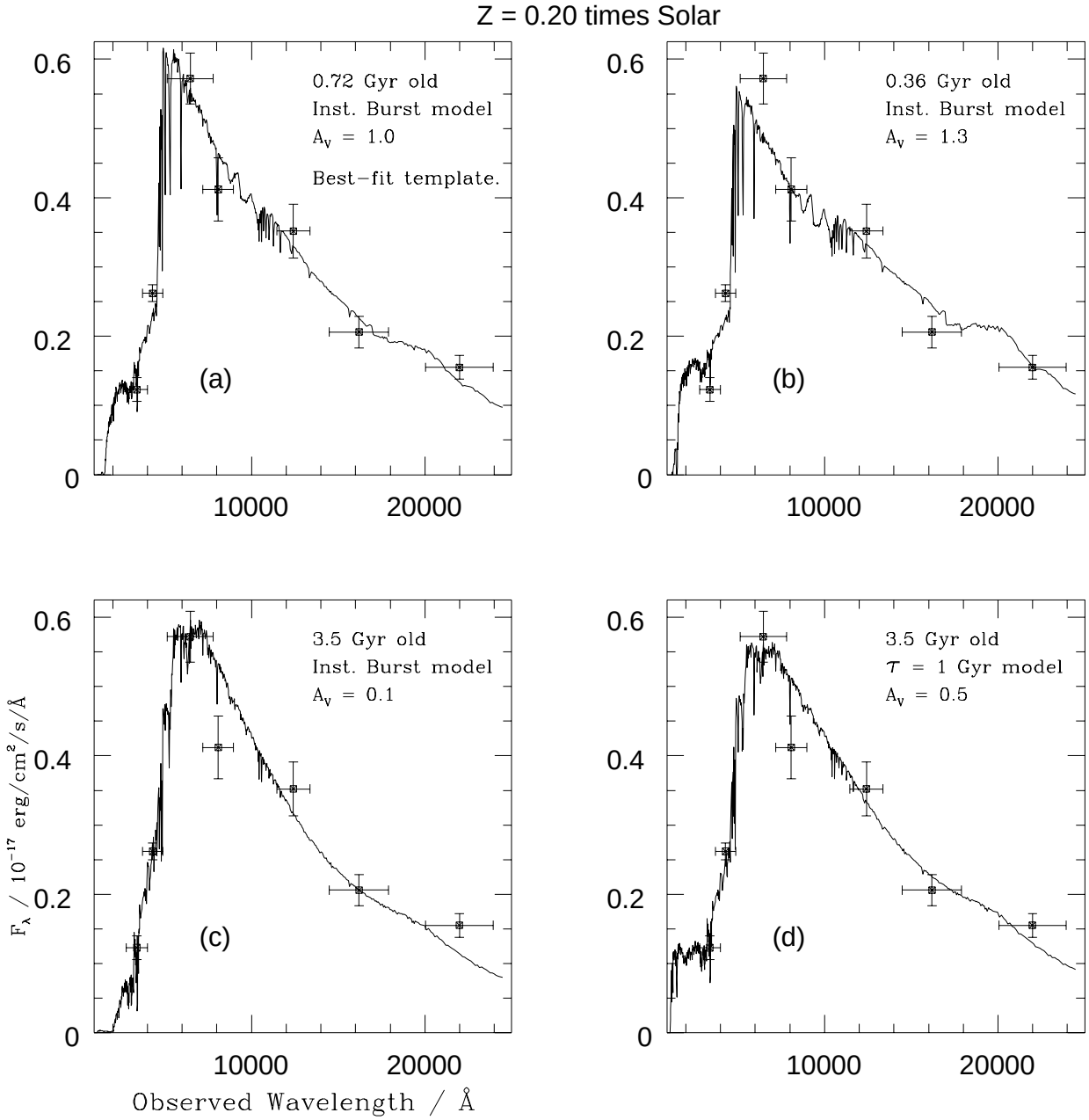

Fig. 4.— Photometry of G1 ($z = 0.22$) corrected for Galactic reddening ($A_B = 0.18$) and converted to an f_λ scale showing the agreement between the colors (U, B, R, I, J, H, K) and the 1996 models of Bruzual and Charlot (see Bruzual & Charlot 1993). The four panels are as follows: (a) a 0.72 Gyr old instantaneous-burst model with $A_V = 1.0$, (b) a 0.36 Gyr old instantaneous-burst model with $A_V = 1.3$, (c) a 3.5 Gyr old instantaneous-burst model with $A_V = 0.1$, and (d) a 3.5 Gyr old model with an exponentially decreasing star formation rate ($\tau = 1$ Gyr and $A_V = 0.5$). All models are 20% solar metallicity and use a Scalo (1986) initial mass function. Panel (a) is the best-fitting model, while the others are acceptable alternatives.

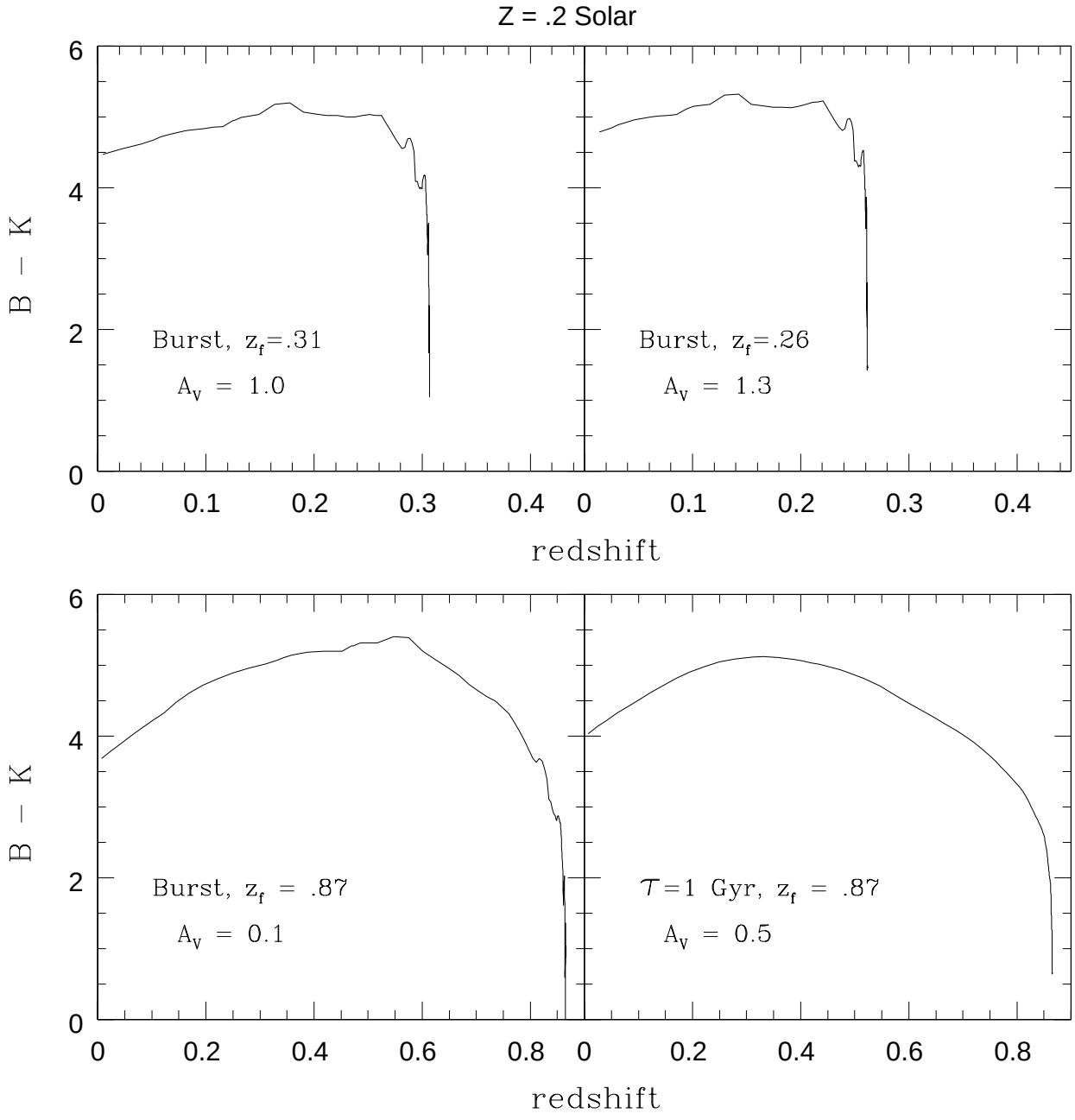

Fig. 5.— Calculated B−K color evolution of G1 ($z = 0.22$) from its formation epoch to the present. Panels a-d correspond to panels a-d in Figure 4, respectively. Dust extinction was assumed constant in the calculation.

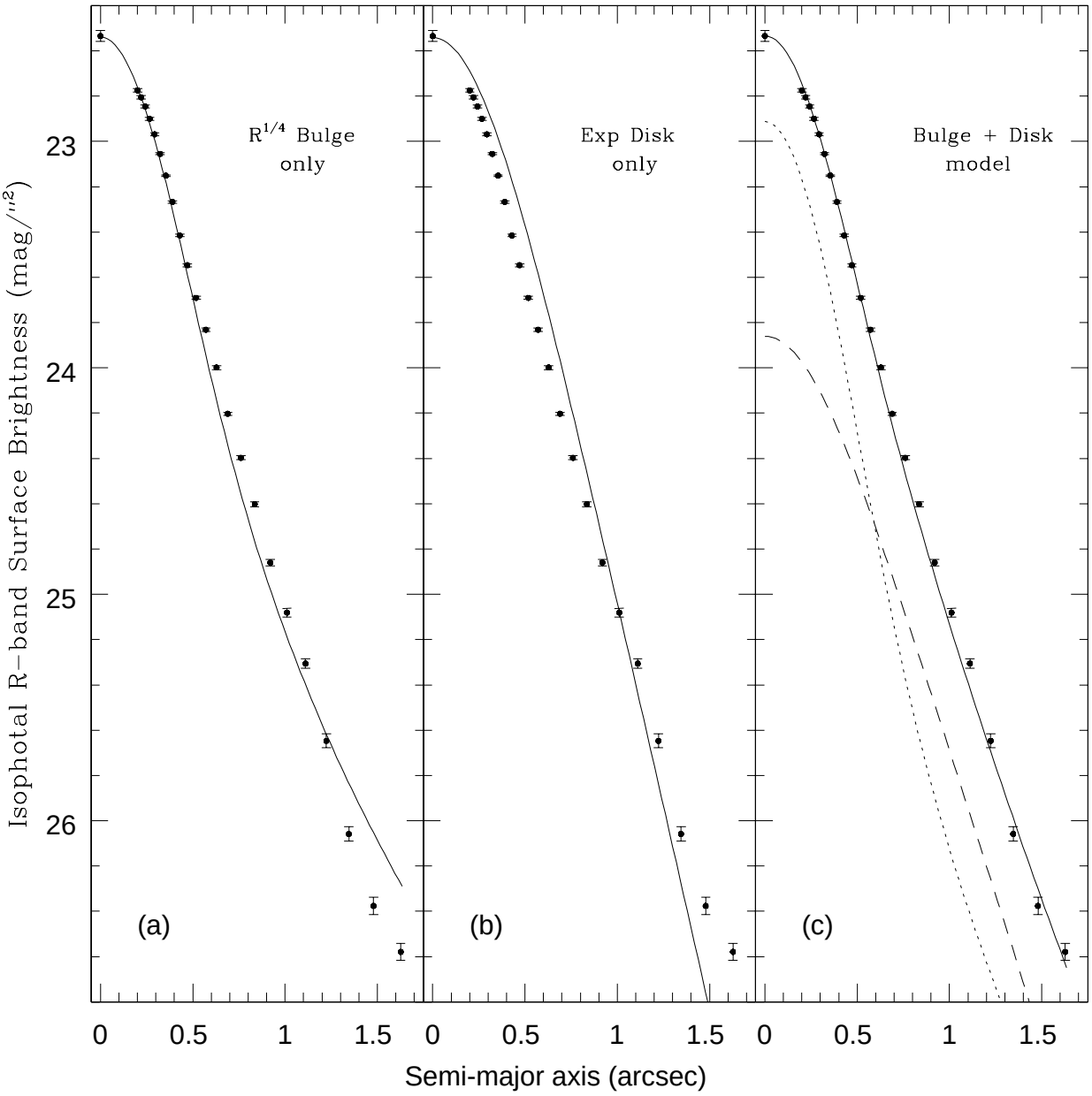

Fig. 6.— Model fits to the the R-band radial light profile of G1: (a) an $r^{1/4}$ (bulge) profile alone, (b) an exponential (disk) profile alone, and (c) the best-fitting model where the interior isophotes are dominated by an $r^{1/4}$ law and the outer isophotes are dominated by an exponential.

Table 1. Journal of Imaging Observations

Filter	Telescope	Observation Date	Exp. Time (m)
U	MDM	1999 Feb 20	60
”	”	1999 Nov 13	90
”	”	1999 Nov 14	60
B	WIYN	1997 Nov 5	30
”	”	1998 Nov 25	15
R	”	1997 Nov 5	45
”	”	1999 Jan 18	15
I	”	1997 Dec 5	50
J	IRTF	1998 Dec 13	30
”	”	1999 Apr 29	63
H	”	1998 Dec 13	30
”	”	2000 Mar 8	63
K	”	1998 Dec 12	130
”	”	1998 Dec 14	132
”	”	1999 Apr 28	63
”	”	2000 Mar 6	126

Table 2. UBRIJHK Photometry[a]

Filter	Limiting mag[b]	G1 Aperture mag	G1 Total mag	G1 μ_0[c]	Jet μ	Arm μ
U	24.7	23.67 (0.15)	22.8 (0.15)	23.8 (0.3)	···	···
B	25.7	23.46 (0.05)	22.7 (0.05)	23.4 (0.2)	···	···
R	27.0	21.49 (0.07)	20.8 (0.05)	21.5[d](0.1)	25.1 (0.2)	···
I	24.1	21.07 (0.12)	20.4 (0.1)	21.0 (0.1)	···	···
J	22.8	19.82 (0.12)	18.9 (0.1)	19.9 (0.1)	22.1 (0.5)	···
H	21.0	19.38 (0.12)	18.7 (0.1)	19.6 (0.1)	···	···
K	22.5	18.52 (0.12)	17.8 (0.1)	18.3[e](0.1)	21.9 (0.2)	21.5 (0.2)

[a]corrected for Galactic extinction

[b]2-σ detection limit in 1.4 arcsec aperture

[c]central surface brightness at 1 arcsec resolution

[d]20.6 at 0.55 arcsec resolution

[e]17.8 at 0.75 arcsec resolution